

12. J. P. Sleeman, J. Krishnan, V. Kirkin, P. Baumann, *Microsc. Res. Tech.* **55**, 61 (2001).
13. Lymphatic vessels were classified as follows: normal tissue lymphatics (NTL); tumor margin lymphatics (TML), found within 150 μm of the surface of skin overlying the tumor; and intratumor lymphatics (ITL), found farther than 150 μm from the surface of the overlying the tumor. The 150- μm delineation comes from the addition of $\sim 50 \mu\text{m}$ for the thickness of the skin and 100 μm , designated as the tumor margin in previous studies (5).
14. MECA-32 may not stain 100% of vascular and lymphatic endothelium.
15. R. K. Jain, *Sci. Am.* **271**, 58 (July 1994).
16. M. Skobe et al., *Am. J. Pathol.* **159**, 893 (2001).
17. G. W. Schmid-Schonbein, *Physiol. Rev.* **70**, 987 (1990).
18. T. P. Padera, B. S. Stoll, P. T. C. So, R. K. Jain, *Mol. Imaging* **1**, 9 (2002).
19. E. B. Brown et al., *Nature Med.* **7**, 864 (2001).
20. VEGF-C was shown qualitatively to increase the size of peritumor LYVE-1-stained vessels in (16).
21. Only three ITLs were found. One ITL per tumor was found in 3 of 14 tumors at depths of 160 μm (MT), 200 μm (VEGF-C), and 260 μm (VEGF-C).
22. M. Jeltsch et al., *Science* **276**, 1423 (1997).
23. E. K. Rofstad et al., *Cancer Res.* **62**, 661 (2002).
24. J. Trzewik, S. K. Mallipattu, G. M. Artmann, F. A. Delano, G. W. Schmid-Schonbein, *FASEB J.* **15**, 1711 (2001).
25. G. Helmlinger, P. A. Netti, H. C. Lichtenfeld, R. J. Melder, R. K. Jain, *Nature Biotechnol.* **15**, 778 (1997).
26. S. J. Mandriota et al., *EMBO J.* **20**, 672 (2001).
27. M. Skobe et al., *Nature Med.* **7**, 192 (2001).
28. T. Karpanen et al., *Cancer Res.* **61**, 1786 (2001).
29. T. Makinen et al., *EMBO J.* **20**, 4762 (2001).
30. R. K. Jain, T. P. Padera, *J. Natl. Cancer Inst.* **94**, 785 (2002).
31. We thank D. Jackson, S. Tomarev, K. Alitalo, B. Seed,

P. So, and A. Hartford for reagents and advice; S. Roberge, P. Huang, C. Swandal, D. Capen, and R. Delgiacco for outstanding technical support; and D. Fukumura, B. Fenton, and B. Stoll for discussion. Supported by NIH (Bioengineering Research Partnership Grant R24-CA85140). T.P.P. received an NSF Graduate Fellowship.

Supporting Online Material
www.sciencemag.org/cgi/content/full/1071420/DC1
Materials and Methods
SOM Text
Figs. S1 to S4
Tables S1 and S2

28 February 2002; accepted 29 March 2002
Published online 25 April 2002;
10.1126/science.1071420
Include this information when citing this paper.

Structure of an HIF-1 α -pVHL Complex: Hydroxyproline Recognition in Signaling

Jung-Hyun Min,¹ Haifeng Yang,² Mircea Ivan,² Frank Gertler,⁴ William G. Kaelin Jr.,^{2,3} Nikola P. Pavletich^{1*}

The ubiquitination of the hypoxia-inducible factor (HIF) by the von Hippel-Lindau tumor suppressor (pVHL) plays a central role in the cellular response to changes in oxygen availability. pVHL binds to HIF only when a conserved proline in HIF is hydroxylated, a modification that is oxygen-dependent. The 1.85 angstrom structure of a 20-residue HIF-1 α peptide-pVHL-ElonginB-ElonginC complex shows that HIF-1 α binds to pVHL in an extended β strand-like conformation. The hydroxyproline inserts into a gap in the pVHL hydrophobic core, at a site that is a hotspot for tumorigenic mutations, with its 4-hydroxyl group recognized by buried serine and histidine residues. Although the β sheet-like interactions contribute to the stability of the complex, the hydroxyproline contacts are central to the strict specificity characteristic of signaling.

The cellular response to oxygen is a central process in animal cells and figures prominently in the pathophysiology of several diseases, including cancer, cardiovascular disease, and stroke (1). This process is coordinated by the hypoxia-inducible factor (HIF) and its regulator, the von Hippel-Lindau tumor suppressor protein (pVHL) (2, 3). HIF is a heterodimeric transcription factor that activates the expression of genes involved in angiogenesis, erythropoiesis, energy metabolism, apoptosis, and/or proliferation in response to low-oxygen tension (hypoxia) conditions. pVHL inhibits HIF activity under normal oxygen conditions (normoxia) by targeting the HIF α subunits for polyubiquitina-

tion and proteasomal degradation (4-8). Under hypoxic conditions the HIF α subunits are not recognized by pVHL, and they consequently accumulate and dimerize with HIF-1 β (2, 3). *VHL* is mutated in the von Hippel-Lindau cancer predisposition syndrome and in sporadic clear-cell renal carcinomas, and this is associated with constitutively high levels of HIF-1 α and the development of highly vascularized tumors (2).

pVHL is the substrate-recognition subunit of a ubiquitin-protein ligase that also contains ElonginB, ElonginC, Cul2, and Rbx1 (VBC-CR complex) (6-9). VBC-CR and the related Skp1-Cul1-F-box (SCF) family of ubiquitin-protein ligases (10) catalyze the transfer of ubiquitin from a ubiquitin-conjugating enzyme to specific lysine residues on the substrate (11).

pVHL binding to HIF-1 α is dependent on the hydroxylation of a core proline residue (Pro⁵⁶⁴) within the HIF-1 α oxygen-dependent degradation domain (ODD) (12-14). This modification is carried out by recently identified HIF prolyl hydroxylases (HPHs) only in the presence of oxygen (15-17). A

20-residue HIF-1 α ODD region (destruction sequence), conserved in animal orthologs and paralogs, is necessary and sufficient for hydroxylation by HPHs and for binding to pVHL (12, 13).

To investigate the targeting of HIF-1 α by the VBC-CR ubiquitin-protein ligase and the basis of hydroxyproline recognition in intracellular signaling, we determined the 1.85 Å crystal structure of the pVHL-ElonginB-ElonginC (VBC) complex bound to the hydroxyproline-containing 20-residue destruction sequence of HIF-1 α (Table 1 and fig. S1). The structure shows that a 15-amino acid portion of HIF-1 α (residues 561 to 575) adopts an extended, β strand-like conforma-

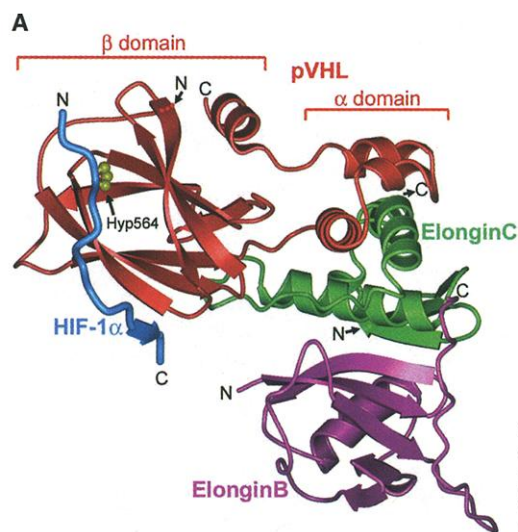
Table 1. Statistics from the crystallographic analysis. Details of the crystallization and structure determination are provided in the supplementary material (22). The statistics for the outermost shell, 1.92 to 1.85 Å, are shown in parentheses. rmsd, Root mean square deviations from ideal geometry and root mean square variation in the B-factor of bonded atoms.

Parameter	Data
Beam line	MacCHESS F1
Resolution (Å)	1.85
Observations	248,351
Unique reflections	34,115
Data coverage (%) (last shell, 1.92-1.85)	88.7 (76.5)
R_{sym}^* (%) (last shell, 1.92-1.85)	7.9 (38.2)
<i>Refinement statistics (15.0-1.85)</i>	
Reflections ($ F > 0\sigma$)	33,935
Total atoms	3409
Water atoms	523
R-factor \dagger (%) (last shell, 1.92-1.85)	19.6 (24.8)
R_{free}^\ddagger (%) (last shell, 1.92-1.85)	23.6 (29.3)
rmsd bonds (Å)	0.007
rmsd angles ($^\circ$)	1.40
rmsd B-factor (Å^2)	3.7

* $R_{\text{sym}} = \sum_p \sum_i |I_{h,j} - I_h| / \sum_p \sum_i I_{h,j}$ for the intensity (I) of i observations of reflection h . $\dagger R$ factor = $\sum |F_o| - |F_c| / \sum |F_o|$, where F_o and F_c are the observed and calculated structure factors, respectively. $\ddagger R_{\text{free}} = R$ factor calculated using 5% of the reflection data chosen randomly and omitted from the start of refinement.

¹Cellular Biochemistry and Biophysics Program and Howard Hughes Medical Institute, Memorial Sloan-Kettering Cancer Center, New York, NY 10021, USA. ²Dana-Farber Cancer Institute and ³Howard Hughes Medical Institute, Harvard Medical School, Boston, MA 02115, USA. ⁴Department of Biology, Massachusetts Institute of Technology, Cambridge, MA 02139, USA.

*To whom correspondence should be addressed. E-mail: nikola@xray2.mskcc.org.



B

	560	N segment	570	C segment																			
556	DL	LDLEMLAPYI	--PMDD	DFQLR	1st Destruction Sequence																		
569	DL	LDLEMLAPYI	--PMDD	DFQLR	human HIF-1α																		
552	DL	LDLEMLAPYI	--PMDD	DFQLR	mouse HIF-1α																		
842	FE	AFAMRAPYI	--PI	DD-MP	LL	frog HIF-1α																	
613	EP	DLSC	LAPFV	--DTYD	MMQMD	fly HIF-1α																	
523	EL	DLETLAPYI	--PMD	GEDFQ	LS	worm HIF-1																	
522	EL	DLETLAPYI	--PMD	GEDFQ	LS	human HIF-2α																	
482	AL	DLEMLAPYI	--SMDD	DFQLN		mouse HIF-2α																	
479	TL	DLEMLAPYI	--SMDD	DFQLN		human HIF-3α																	
					mouse HIF-3α																		
394	PD	AL	TL	L	L	AP	A	AG	D	T	I	I	S	L	D	F	G	S	N	2nd Destruction Sequence			
394	PD	AL	TL	L	L	AP	A	AG	D	T	I	I	S	L	D	F	G	S	N	human HIF-1α			
397	PE	E	L	A	Q	L	A	P	T	P	G	D	A	I	I	S	L	D	F	G	S	N	mouse HIF-1α
397	PE	E	L	A	Q	L	A	P	T	P	G	D	A	I	I	S	L	D	F	G	S	N	human HIF-2α
397	PE	E	L	A	Q	L	A	P	T	P	G	D	A	I	I	S	L	D	F	G	S	N	mouse HIF-2α

orthologs are aligned below. The reported second destruction sequence is 38 residues long, and only a 23-residue region that aligns with the first destruction sequence is shown. Dashes indicate gaps relative to the seven-residue spacing between the putative N and C segments of the second destruction sequence.

tion (Fig. 1A). It binds pVHL in a bipartite manner, with two discontinuous HIF-1α segments interacting with a continuous site on pVHL. A six-residue NH₂-terminal segment (residues 561 to 566; N segment) that is centered on Hyp⁵⁶⁴ (Hyp is the three-letter code for hydroxyproline), and a four-residue COOH-terminal segment (residues 571 to 574; C segment) are separated by a four-amino acid bulge that does not contact pVHL (Fig. 1B). Complex formation brings a total of 1960 Å² surface area, 63% of which is due to the N segment. The NH₂-terminal five amino acids (residues 556 to 560) of the peptide are disordered.

pVHL has two tightly coupled domains consisting of a ~100-amino acid β sandwich (β domain), and a ~35-amino acid three-helix cluster (α domain) (10). The α domain binds ElonginC, which, in association with ElonginB, recruits the VBC complex to Cul2-Rbx1 to form the ubiquitin-protein ligase (8–10). HIF-1α interacts exclusively with the β domain of pVHL. It binds alongside the β sandwich, making five backbone-backbone hydrogen bonds (Fig. 1A). The side of the pVHL β sandwich where HIF-1α binds has the hydrophobic core partially exposed. This exposed hydrophobic patch, together with several partially buried polar residues, makes up the binding site of the hydroxyproline.

The hydroxyproline has a central role in complex formation. It is nearly entirely buried, with 96% of its accessible surface area in a hypothetical free peptide covered by pVHL. The pyrrolidine ring inserts toward the partially exposed hydrophobic core of the pVHL β domain, making multiple van der Waals contacts with Trp⁸⁸, Tyr⁹⁸, and Trp¹¹⁷ of pVHL (Fig. 2A). The 4-hydroxyl group in-

teracts farthest into pVHL and forms hydrogen bonds with the Nδ of His¹¹⁵ (2.7 Å) and the OH group of Ser¹¹¹ (2.7 Å), both of which also form hydrogen bonds with other pVHL groups (Fig. 2A). His¹¹⁵ and Ser¹¹¹ are partially solvent exposed in the apo-VBC structure (10) but become entirely buried on HIF-1α binding. If Pro⁵⁶⁴ were not hydroxylated, HIF-1α binding would result in the desolvation of His¹¹⁵ and Ser¹¹¹ without the replace-

Fig. 1. The HIF-1α destruction sequence binds the β domain of pVHL in an extended β strand-like conformation. (A) Schematic representation of the 15-residue portion of the HIF-1α destruction sequence bound to the β domain of pVHL in the pVHL–ElonginB–ElonginC complex. The portion of HIF-1α that adopts a continuous β-strand conformation is indicated by a wide arrow. HIF-1α is in blue, Hyp⁵⁶⁴ in yellow, pVHL in red, ElonginB in magenta, and ElonginC in green. C, COOH-terminus; N, NH₂-terminus. The figures are prepared with MOLSCRIPT (27), GL_RENDER, and POVRAY (28). (B) Alignment of the first destruction sequence in the ODDs of HIF-1α orthologs and HIF-2α and HIF-3α paralogs, highlighting residues identical in seven of the nine sequences. The N and the C segments of human HIF-1α are indicated in red. The putative N and C segments of the second destruction sequences of HIF-1α and HIF-2α

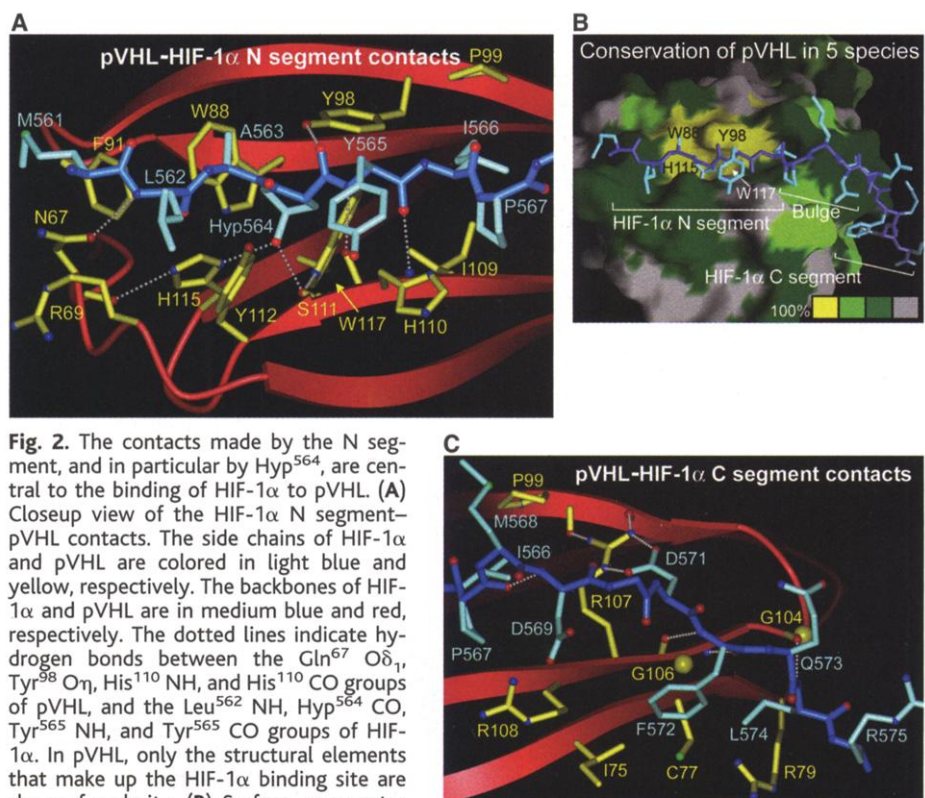


Fig. 2. The contacts made by the N segment, and in particular by Hyp⁵⁶⁴, are central to the binding of HIF-1α to pVHL. (A) Closeup view of the HIF-1α N segment–pVHL contacts. The side chains of HIF-1α and pVHL are colored in light blue and yellow, respectively. The backbones of HIF-1α and pVHL are in medium blue and red, respectively. The dotted lines indicate hydrogen bonds between the Gln⁵⁷ Oδ₁, Tyr⁹⁸ Oη, His¹¹⁰ NH, and His¹¹⁰ CO groups of pVHL, and the Leu⁵⁶² NH, Hyp⁵⁶⁴ CO, Tyr⁵⁶⁵ NH, and Tyr⁵⁶⁵ CO groups of HIF-1α. In pVHL, only the structural elements that make up the HIF-1α binding site are shown for clarity. (B) Surface representation of pVHL colored according to the degree of conservation in the pVHL orthologs in Fig. 1B. Yellow indicates identity in five orthologs (labeled residues), light green in four, and dark green in three. The HIF-1α side chains are in light blue, and the backbone is in medium blue. The N segment is in an orientation similar to that of (A). The approximate boundaries of the N and C segments and of the bulge are indicated. (C) Closeup view of the bulge and the C-segment area of the HIF-1α peptide–pVHL complex. The 567 P-M-D-D 571 bulge sequence does not contact pVHL, but forms an intramolecular β-turn hydrogen bond (CO of Pro⁵⁶⁷ and NH of Asp⁵⁶⁹). The Asp⁵⁷⁰ side chain of HIF-1α is omitted for clarity.

tially solvent exposed in the apo-VBC structure (10) but become entirely buried on HIF-1α binding. If Pro⁵⁶⁴ were not hydroxylated, HIF-1α binding would result in the desolvation of His¹¹⁵ and Ser¹¹¹ without the replace-

ment.

REPORTS

ment of the lost interactions between these side chains and water. This would be an energetically unfavorable process. His¹¹⁵ and Ser¹¹¹ are thus likely to be key determinants of the strict requirement for the hydroxylation of Pro⁵⁶⁴.

The pVHL residues that interact with Hyp⁵⁶⁴ are highly conserved in the human, mouse, frog, fly, and worm pVHL orthologs (Fig. 2B). Trp⁸⁸, Tyr⁹⁸, His¹¹⁵, and Trp¹¹⁷ are among the 11 β domain residues that are invariant in the five orthologs, and Ser¹¹¹ is replaced with a threonine in the frog, fly, and worm (fig. S2). Mutations of Tyr⁹⁸, Ser¹¹¹, and Trp¹¹⁷ of pVHL have been shown to abolish HIF-1 α binding (18).

The backbone of HIF-1 α in the vicinity of Hyp⁵⁶⁴ is held in place through an extensive network of hydrogen bonds involving both backbone and side-chain groups from pVHL (Fig. 2A). These interactions are likely to increase the specificity at the hydroxyproline-binding site of pVHL by limiting the conformational flexibility of the HIF-1 α backbone.

Compared with Hyp⁵⁶⁴, the other N-segment residues make significantly fewer contacts. Among them, Ile⁵⁶⁶ makes the most contacts, interacting with Pro⁹⁹ and Ile¹⁰⁹ of pVHL. Met⁵⁶¹ packs with Phe⁹¹ of pVHL, Leu⁵⁶² with Tyr¹¹² and Arg⁶⁹, Ala⁵⁶³ with Trp⁸⁸, and Tyr⁵⁶⁵ with His¹¹⁰ (Fig. 2A). These side-chain contacts occur on the surface of the complex, however, and are unlikely to make a major contribution to specificity and affinity compared with Hyp⁵⁶⁴. This conclusion is consistent with the observations that mutation of Met⁵⁶¹ (12) or Leu⁵⁶² (12, 16) to alanine does

not affect pVHL binding, and mutation of Ala⁵⁶³ to glycine (16) or Tyr⁵⁶⁷ to alanine (13, 16) reduces but does not abolish binding in the context of a hydroxylated peptide. These mutations prevent the hydroxylation of HIF-1 α , however, suggesting that the overall high conservation of these residues (Fig. 1B) is due to their role in HPH binding (12, 16). Similarly, the conservation of residues 556 to 560 (Fig. 1B), which are disordered in the structure, may be due to their involvement in HPH binding. That HPH binding appears to involve more side chains of HIF-1 α compared with pVHL binding (12, 13, 16, 18) may reflect the reliance of pVHL on the presence of the relatively rare hydroxyproline amino acid for its recognition of HIF-1 α . HPHs would have to rely solely on recognizing canonical amino acids.

The N segment is followed by Pro⁵⁶⁷, which directs the chain away from pVHL. Pro⁵⁶⁷ and the next three residues form a bulge, which, although visible in the electron density map, does not contact pVHL. The bulge could, in principle, be as short as two nonproline residues and also could be substantially longer and still allow the N and C segments to interact with pVHL (supporting online text). A second, independent destruction sequence within the HIF-1 α ODD (19) may interact with pVHL in a similar mode if we assume seven instead of four residues in the bulge between its putative hydroxyproline-containing N-segment- and C-segment-like sequences (Fig. 1B).

The C segment following the bulge adopts a β -strand conformation and makes three backbone-backbone hydrogen bonds,

as well as side-chain contacts to pVHL (Fig. 2C). The Asp⁵⁷¹ side chain of HIF-1 α hydrogen bonds with the Arg¹⁰⁷ side chain of pVHL, Phe⁵⁷² makes van der Waals contacts to Ile⁷⁵ and Gly¹⁰⁶, and Leu⁵⁷⁴ contacts Cys⁷⁷ and Arg⁷⁹ (Fig. 2C). Overall, these contacts are solvent exposed on the surface of the complex, and the HIF-1 α and pVHL residues involved are not as conserved as those in the N-segment portion of the interface (Figs. 1B, 2B, and fig. S2). This suggests that the C-segment side-chain contacts are not as important for pVHL binding.

This conclusion is supported by the distribution of VHL tumor-derived missense mutations (20), which tend to cluster at the Hyp⁵⁶⁴ binding site of pVHL. All of the five pVHL residues that contact Hyp⁵⁶⁴ are mutated at high frequencies (Fig. 3 and fig. S2). In fact, Tyr⁹⁸, whose side chain is not important for the structural integrity of the β sandwich (10, 21) but which contacts both the pyrrolidine ring and backbone carbonyl group of Hyp⁵⁶⁴, is the second most frequently mutated amino acid of pVHL (the first one, Arg¹⁶⁷, maps to the α - β interdomain interface). In contrast, the pVHL residues that contact the HIF-1 α C segment are either not mutated or mutated at low frequencies (Fig. 3 and fig. S2).

To further investigate the relative importance of the N and C segments, we used isothermal titration calorimetry (ITC) to measure the affinities of the intact, N-segment and C-segment peptides for pVHL (22). We found that the intact peptide bound pVHL with a dissociation constant (K_d) of $0.22 \pm 0.04 \mu\text{M}$; the N-segment peptide bound with one-third the affinity, K_d of $0.61 \pm 0.10 \mu\text{M}$ (Table 2 and fig. S3). We could not detect an interaction with the nonhydroxylated intact peptide under the same conditions. The C-segment peptide exhibited binding only at

Fig. 3. The Hyp⁵⁶⁴ binding site is a hotspot of tumorigenic pVHL mutations. Surface representation of the pVHL β domain colored according to the frequency of tumorigenic missense mutations. The current universal VHL-mutation database contains 363 tumor-derived missense mutations, 210 of which map to the β domain residues 60 to 153. Mutation frequencies >4% are shown in yellow, <4% and >2% in orange, <2% and >1% in red. Mutations at residues that contact Hyp⁵⁶⁴ account for 21% of the β domain mutations, while those at residues that contact the C segment account for 2%, and these are limited to the Gly¹⁰⁴-Thr¹⁰⁵-Gly¹⁰⁶ sequence that makes backbone-backbone hydrogen bonds to HIF-1 α . The rest map to residues that have structural roles in the hydrophobic core or in turns between β strands.

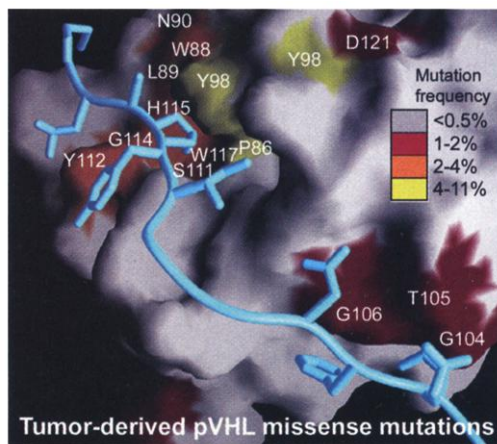


Table 2. Thermodynamic parameters of HIF-1 α -pVHL binding.

Parameter	ΔH (kcal/mol)	$T\Delta S$ (kcal/mol)	ΔG (kcal/mol)	K_d (μM)
Intact peptide*	-18.0 ± 0.2	-8.9 ± 0.2	-9.1 ± 0.05	0.22 ± 0.04
N segment†	-7.2 ± 0.1	1.3 ± 0.2	-8.5 ± 0.05	0.61 ± 0.10
C segment*	-13.4 ± 3.4	-9.6 ± 2.0	-4.4 ± 0.1	536 ± 57

*Thermodynamic parameters and errors from two independent experiments. †From three independent experiments.

Peptide	Sequence	VBC far-Western
N0	DLEMLAXYIPMD	+
N1	LEMLAXYIPMD	+
N2	EMLAXYIPMD	+
N3	MLAXYIPMD	+
N4	LAXYIPMD	+
N5	AXYIPMD	+/-
N6	XYIPMD	-
N7	DLEMLAXYIPM	+
N8	DLEMLAXYIP	+
N9	DLEMLAXYI	+
N10	DLEMLAXY	-

Fig. 4. Summary of pVHL far-Western assay with HIF-1 α peptides lacking the C segment. The N-segment residues in the vicinity of Hyp⁵⁶⁴ have secondary roles in binding and specificity. Owing to variations in the amounts of the peptides on the filter, a more quantitative determination is not possible. X indicates hydroxyproline.

very high concentrations with a K_d of $536 \pm 57 \mu\text{M}$ (Table 2 and fig. S3).

We next investigated the minimal portion of the N segment required for pVHL binding with a far-Western assay (18, 22). Using a peptide lacking the C segment as reference (peptide N0 in Fig. 4 and fig. S4A), we found that deletion of the NH_2 -terminal residues that are disordered in the crystal structure (N1 to N3) and of Met^{561} (N4) had no significant effect. Deletion of Leu^{562} (N5) reduced binding, and further deletion of Ala^{563} (N6) eliminated binding, possibly as a cumulative effect of eliminating the contacts made by Met^{561} , Leu^{562} , and Ala^{563} . COOH-terminal deletions of the bulge residues (N7 to N9) had no effect, but deletion of Ile^{566} (N10) drastically reduced binding, consistent with the more extensive contacts made by Ile^{566} than those of Met^{561} , Leu^{562} , or Ala^{563} . Using the same far-Western assay, we found that the only amino acid that could weakly substitute for the hydroxyproline was cysteine (fig. S4B).

Taken together, the structural, thermodynamic, and mutational data indicate that the primary contribution to specificity and affinity is provided by the hydroxyproline side chain, with only secondary contributions from the other side chains in the N segment and an overall minor contribution to affinity from the entire C segment.

The mammalian HPHs have been suggested to contain a jelly roll β -barrel structure and active-site characteristics in common with other iron and 2-oxoglutarate-dependent oxygenases (17, 23, 24). In these enzymes (25), iron, 2-oxo-

glutarate, and substrates are bound in a spacious cavity, which is located between the two sheets of the jelly roll and is exposed at one side of the β barrel. Although topologically different, the architecture and position of this active-site cavity are reminiscent of the hydroxyproline-binding site of the pVHL β sandwich, leading to the model that HIF-1 α may bind to HPHs by forming an intermolecular β sheet and inserting the proline side chain into the β -barrel cavity.

In contrast to extracellular proteins where hydroxyproline plays a structural role (26), the hydroxyproline in HIF-1 α is a central determinant of signaling, and the structure of the HIF-1 α -VBC complex reveals how it can be recognized with the strict specificity that is characteristic of signaling. The structure also provides a framework for the discovery of inhibitors that prevent HIF-1 α degradation and promote therapeutic angiogenesis in cardiovascular disease and stroke.

References and Notes

- G. L. Semenza, *Genes Dev.* **14**, 1983 (2000).
- M. Ivan, W. G. Kaelin Jr., *Curr. Opin. Genet. Dev.* **11**, 27 (2001).
- R. K. Bruick, S. L. McKnight, *Genes Dev.* **15**, 2497 (2001).
- L. E. Huang, J. Gu, M. Schau, H. F. Bunn, *Proc. Natl. Acad. Sci. U.S.A.* **95**, 7987 (1998).
- P. H. Maxwell et al., *Nature* **399**, 271 (1999).
- K. Iwai et al., *Proc. Natl. Acad. Sci. U.S.A.* **96**, 12436 (1999).
- T. Kamura et al., *Science* **284**, 657 (1999).
- L. Lisztwan, G. Imbert, C. Wirbelauer, M. Gstaiger, W. Krek, *Genes Dev.* **13**, 1822 (1999).
- A. Pause et al., *Proc. Natl. Acad. Sci. U.S.A.* **94**, 2156 (1997).
- C. E. Stebbins, W. G. Kaelin Jr., N. P. Pavletich, *Science* **284**, 455 (1999).

- R. J. Deshaies, *Annu. Rev. Cell. Dev. Biol.* **15**, 435 (1999).
- M. Ivan et al., *Science* **292**, 464 (2001).
- P. Jaakkola et al., *Science* **292**, 468 (2001).
- F. Yu, S. B. White, Q. Zhao, F. S. Lee, *Proc. Natl. Acad. Sci. U.S.A.* **98**, 9630 (2001).
- G. L. Semenza, *Cell* **107**, 1 (2001).
- R. K. Bruick, S. L. McKnight, *Science* **294**, 1337(2001).
- A. C. Epstein et al., *Cell* **107**, 43 (2001).
- M. Ohh et al., *Nat. Cell Biol.* **2**, 423 (2000).
- N. Masson, C. Willam, P. H. Maxwell, C. W. Pugh, P. J. Ratcliffe, *EMBO J.* **20**, 5197 (2001).
- C. Beroud et al., *Nucleic Acids Res.* **26**, 256 (1998).
- M. Ohh et al., *J. Clin. Invest.* **104**, 1583 (1999).
- Materials and methods are available as supporting material on Science Online.
- L. Aravind, E. V. Koonin, *Genome Biol.* **2** (2001).
- M. S. Taylor, *Gene* **275**, 125 (2001).
- I. J. Clifton, L. C. Hsueh, J. E. Baldwin, K. Hartos, C. J. Schofield, *Eur. J. Biochem.* **268**, 6625 (2001).
- J. Emsley, C. G. Knight, R. W. Farndale, M. J. Barnes, R. C. Liddington, *Cell* **101**, 47 (2000).
- P. J. Kraulis, *J. Appl. Crystallogr.* **24**, 946 (1991).
- L. Essar, personal communication.
- We thank P. Jeffrey for help with data collection and processing, C. E. Stebbins and the members of the Pavletich lab for helpful discussions, C. Murray and M. Minto for administrative assistance, J. Crawford for peptide synthesis, and the staff of the Cornell High Energy Synchrotron Source for help with data collection. This work was supported by the NIH, the Howard Hughes Medical Institute, the Dewitt Wallace Foundation, the Samuel and May Rudin Foundation, and the Arthur and Rochelle Belfer Foundation. Coordinates have been deposited in the RCSB Protein Data Bank (accession code 1LM8).

Supporting Online Material

www.sciencemag.org/cgi/content/full/1073440/DC1
Materials and Methods
Figs. S1 to S4

8 March 2002; accepted 1 May 2002

Published online 9 May 2002;

10.1126/science.1073440

Include this information when citing this paper.

Learn from the Past, Reach for the Future

AAAS members get the best of both worlds!

Science Archives lets you search our issues back to the very first in 1880. *Science Express* gives you cutting-edge research online weeks before print publication in your personal copy of *Science*.

All this and more is available on AAASMember.org free to individual AAAS members only.

All with the click of a mouse—when you need it and where you need it.

AAAS and *Science*, where science has been, and where science will go.

promo.aaas.org/getscience